

Two-component boson systems with hyperspherical coordinates

T Sogo, O Sørensen, A S Jensen and D V Fedorov

Department of Physics and Astronomy, University of Aarhus, DK-8000 Aarhus C, Denmark

E-mail: taka@phys.au.dk

Abstract. The effective potential is computed for two boson systems in one trap as a function of their two individual hyperadii and the distance between their centers. Zero-range interactions are used and only relative s -states are included. Existence and properties of minima are investigated as a function of these three collective coordinates. For sufficiently strong repulsion stable structures are found at a finite distance between the centers. The relative center of masses motion corresponds to the lowest normal mode. The highest normal mode is essentially the breathing mode where the subsystems vibrate by scaling their radii in phase. The intermediate normal mode corresponds to isovector motion where the subsystems vibrate by scaling their radii in opposite phase. Stability conditions are established as substantially more restrictive than in mean-field computations.

Submitted to: *J. Phys. B: At. Mol. Opt. Phys.*

PACS numbers: 31.15.Ja, 21.45.+v, 05.30.Jp

1. Introduction

Condensed states of identical bosons at zero temperature in a confining external field are accessible for experiments in many laboratories [1, 2]. Most often the condensates are formed by one species of bosons, but also two-component structures have been investigated. The two components may consist of the same atom in two different spin states as studied for ^{87}Rb [3, 4]. The spin states may then be converted from one to the other while maintaining the total number of atoms. Also collective oscillations can be studied experimentally as in [5] for ^{87}Rb . Two-component boson condensates of different atoms have other properties as investigated by combining ^{87}Rb and ^{41}K [6]. More recently mixtures of boson and fermion systems have been realized [7, 8, 9, 10, 11].

The theory for two-component condensates are mostly based on the mean-field approximation [1, 2]. The additional degrees of freedom lead to spatial symmetry breaking in a cylindrical trap as shown in [12, 13]. Collective excitations in such traps are predicted [14]. With two different trap frequencies also spherical traps allow collective excitations [15]. The spatial asymmetry is sometimes favored even in spherical traps [16]. Repulsion between the two components can lead to separation of the two components both in the ground state and for the collective oscillations [17]. Stability conditions can be derived from properties of the collective modes [18].

Another type of formulation using hyperspherical coordinates for one-component boson systems was introduced in [19]. This formulation was extended to include two-body correlations for one-component N -body boson systems [20]. This treatment allowed both very large scattering lengths and attractive two-body interactions. The mathematical collapse is prevented by a finite range interaction. Conditions for the physical collapse are rather similar to mean-field results. Still the computed correlated structures for large scattering length may be physically interesting [21].

The present paper follows up with more details and new calculations on a recent attempt to extend the hyperspherical formulation to two-component boson systems [22]. Although several new features appear, we still only employ the lowest-order approximation with inclusion of three collective coordinates. This is the minimum number of degrees of freedom which can describe individual sizes of the two subsystems and their separation distance. A demand for more complicated extensions may arise, but the specific direction is better decided after digestion of the results from the simplest model survey.

In section 2 we formulate the theoretical framework where the effective potential is introduced. The properties of this key quantity is investigated in details in section 3, especially with respect to minima and their curvatures. Then we are equipped to establish stability conditions for the total system as discussed in section 4. Our conclusions are contained in section 5. Finally, for completeness we include a number of rather tedious mathematical details in three appendices, but the main text can be read independently because only analytic and numerical results are used.

2. Theoretical formulation

We consider a dilute system of two species of bosons, A and B , with boson masses m_A and m_B and particle numbers N_A and N_B . We label the particles with $i = 1, 2, 3, \dots, N_A$ for component A and $i = N_A + 1, N_A + 2, \dots, N \equiv N_A + N_B$ for component B . The individual masses and position vectors are denoted m_i and \vec{r}_i where $i = 1, 2, 3, \dots, N$. These bosons are trapped in a spherically symmetric harmonic oscillator potential with the same trap frequency ω . The Hamiltonian describing this system is

$$H = H_0 + V_A + V_B + V_{AB} \quad (1)$$

$$H_0 = \sum_{i=1}^{N_A} \left[-\frac{\hbar^2}{2m_A} \vec{\nabla}_i^2 + \frac{1}{2} m_A \omega^2 r_i^2 \right] + \sum_{i=N_A+1}^N \left[-\frac{\hbar^2}{2m_B} \vec{\nabla}_i^2 + \frac{1}{2} m_B \omega^2 r_i^2 \right] \quad (2)$$

$$V_A = \sum_{i>j=1}^{N_A} g_A \delta^{(3)}(\vec{r}_{ij}), \quad g_A = \frac{4\pi\hbar^2 a_A}{m_A}, \quad (3)$$

$$V_B = \sum_{i>j=N_A+1}^N g_B \delta^{(3)}(\vec{r}_{ij}), \quad g_B = \frac{4\pi\hbar^2 a_B}{m_B}, \quad (4)$$

$$V_{AB} = \sum_{i=1}^{N_A} \sum_{j=N_A+1}^N g_{AB} \delta^{(3)}(\vec{r}_{ij}), \quad g_{AB} = \frac{2\pi\hbar^2 a_{AB}}{\mu_{AB}}, \quad (5)$$

where $\vec{r}_{ij} \equiv \vec{r}_i - \vec{r}_j$ denotes the vector distance between two particles and the reduced mass of an A and a B particle is given by $\mu_{AB} \equiv m_A m_B / (m_A + m_B)$. The interaction strengths of the two-body zero-range pseudo potentials, g_A , g_B , and g_{AB} , are related to the s -wave scattering lengths, a_A , a_B , and a_{AB} . This normalization is adopted to provide the correct large-distance behavior of the effective potential in mean-field computations [23].

We shall use hyperspherical coordinates with hyperradii defined for both the individual and the total systems [19, 20], i.e.

$$m\rho^2 \equiv \frac{1}{M} \sum_{i<j}^N m_i m_j r_{ij}^2 = \sum_{i=1}^N m_i r_i^2 - MR^2, \quad (6)$$

$$\rho_A^2 \equiv \frac{1}{N_A} \sum_{i<j}^{N_A} r_{ij}^2, \quad \rho_B^2 \equiv \frac{1}{N_B} \sum_{N_A < i < j}^N r_{ij}^2, \quad (7)$$

$$\vec{R}_A = \frac{1}{N_A} \sum_{i=1}^{N_A} \vec{r}_i, \quad \vec{R}_B = \frac{1}{N_B} \sum_{i=N_A+1}^N \vec{r}_i, \quad (8)$$

where $M \equiv M_A + M_B = N_A m_A + N_B m_B$ is the total mass, m is an arbitrary normalization mass, \vec{R}_A , \vec{R}_B are the individual center of mass coordinates and \vec{R} is the overall center-of-mass coordinate, i.e.

$$\vec{R} = \frac{1}{M} \sum_i m_i \vec{r}_i = \frac{M_A \vec{R}_A + M_B \vec{R}_B}{M}. \quad (9)$$

The center of mass separation of the two components is then given by the coordinate $\vec{r} \equiv \vec{R}_B - \vec{R}_A$. The three length coordinates, ρ_A , ρ_B , and r , are related to ρ by

$$m\rho^2 = m_A\rho_A^2 + m_B\rho_B^2 + m_r r^2, \quad m_r \equiv \frac{M_A M_B}{M_A + M_B}. \quad (10)$$

The remaining coordinates, beside ρ_A , ρ_B , \vec{R} , \vec{r} , are all chosen as (hyper)angles denoted collectively for each system by Ω_A and Ω_B .

The total volume element is then given by

$$\prod_{i=1}^{N_A} d^3 r_i \prod_{i=N_A+1}^N d^3 r_i = N_A^{3/2} N_B^{3/2} \rho_A^{3N_A-4} \rho_B^{3N_B-4} d^3 R r^2 dr d\rho_A d\rho_B d\Omega_r d\Omega_{N_A-1} d\Omega_{N_B-1}, \quad (11)$$

where $d\Omega_r$ is the angular volume element for \vec{r} and $d\Omega_{N_A-1}, d\Omega_{N_B-1}$ accounts for the hyperangles collected in Ω_A and Ω_B , see [20] for precise definitions.

Using these coordinates we rewrite the external harmonic oscillator potentials in the Hamiltonian (1) as

$$\begin{aligned} & \frac{1}{2} m_A \omega^2 \sum_{i=1}^{N_A} \vec{r}_i + \frac{1}{2} m_B \omega^2 \sum_{i=N_A+1}^N \vec{r}_i = \\ & \frac{1}{2} M \omega^2 R^2 + \frac{1}{2} m_r \omega^2 r^2 + \frac{1}{2} m_A \omega^2 \rho_A^2 + \frac{1}{2} m_B \omega^2 \rho_B^2 \\ & = \frac{1}{2} M \omega^2 R^2 + \frac{1}{2} m \omega^2 \rho^2. \end{aligned} \quad (12)$$

Furthermore the kinetic energy operator \hat{T} can also be separated in terms related to total center of mass, relative and intrinsic A and B degrees of freedom, i.e.

$$\hat{T} = -\frac{\hbar^2}{2M} \vec{\nabla}_R^2 - \frac{\hbar^2}{2m_r} \vec{\nabla}_r^2 + \hat{T}_A + \hat{T}_B, \quad (13)$$

where ∇_R and ∇_r are the usual three-dimensional derivatives with respect to the indicated coordinates, \hat{T}_A and \hat{T}_B are the intrinsic kinetic-energy operators expressed by hyperspherical coordinates for each boson system, see [20].

The two-body interactions depend only on relative distances and we can completely separate relative and total center of mass motions. Furthermore, we can separate relative A and B except for the coupling term V_{AB} . The Hamiltonian in equation (1) then becomes

$$H = H_{\text{c.m.}} + H_{\text{rel}}, \quad (14)$$

$$H_{\text{c.m.}} = -\frac{\hbar^2}{2M} \vec{\nabla}_R^2 + \frac{1}{2} M \omega^2 R^2, \quad (15)$$

$$H_{\text{rel}} = T_{\rho_A} + T_{\rho_B} + T_r + \frac{1}{2} m_A \omega^2 \rho_A^2 + \frac{1}{2} m_B \omega^2 \rho_B^2 + \frac{1}{2} m_r \omega^2 r^2 + H_\Omega, \quad (16)$$

$$H_\Omega = \frac{\hbar^2}{2m_A} \frac{\hat{\Lambda}_{N_A-1}^2}{\rho_A^2} + \frac{\hbar^2}{2m_B} \frac{\hat{\Lambda}_{N_B-1}^2}{\rho_B^2} + \frac{\hbar^2}{2m_r} \frac{\hat{L}_r^2}{r^2} + V_A + V_B + V_{AB}, \quad (17)$$

$$T_r = -\frac{\hbar^2}{2m_r} \frac{1}{r} \frac{\partial^2}{\partial r^2} r, \quad (18)$$

$$T_{\rho_A} = -\frac{\hbar^2}{2m_A}\rho_A^{2-3N_A/2}\frac{\partial^2}{\partial\rho_A^2}\rho_A^{3N_A/2-2}, \quad (19)$$

$$T_{\rho_B} = -\frac{\hbar^2}{2m_B}\rho_B^{2-3N_B/2}\frac{\partial^2}{\partial\rho_B^2}\rho_B^{3N_B/2-2}, \quad (20)$$

where \hat{L}_r^2 is the usual angular momentum operator with respect to \vec{r} , and $\hat{\Lambda}_{N_A-1}^2$ and $\hat{\Lambda}_{N_B-1}^2$ consist of first and second order derivatives with respect to the hyperangular degrees of freedom indicated by the indices. This Hamiltonian reduces for $m_A = m_B$ and identical interactions, $g_A = g_B = g_{AB}$, to the one-component system described in [20].

The separable center of mass motion is given by the harmonic oscillator solutions to the Hamiltonian in equation (15). The relative motion can be determined by the hyperspherical adiabatic expansion method where the wave function for fixed values of (ρ_A, ρ_B, r) is expanded on the complete set of eigenfunctions for H_Ω in equation (17). The leading term in the lowest adiabatic channel is expected to consist of the lowest partial waves, where the wave function is independent of all (hyper)angles. This is the assumption valid in the large-distance limit where all particles are far from each other and all directional dependence is averaged out [19, 24]. Then the wave function for the lowest eigenvalue reduces to the form

$$\Psi = \rho_A^{2-3N_A/2}\rho_B^{2-3N_B/2}r^{-1}f(\rho_A, \rho_B, r), \quad (21)$$

where f only depends on the three radial coordinates.

This radial wave function and the corresponding eigenvalue E_{rel} are determined from the Schrödinger equation obtained by combining equations (16) and (21), i.e.

$$\left[-\frac{\hbar^2}{2m_A}\frac{\partial^2}{\partial\rho_A^2} - \frac{\hbar^2}{2m_B}\frac{\partial^2}{\partial\rho_B^2} - \frac{\hbar^2}{2m_r}\frac{\partial^2}{\partial r^2} + U_{\text{eff}}(\rho_A, \rho_B, r)\right]f(\rho_A, \rho_B, r) = E_{\text{rel}}f(\rho_A, \rho_B, r) \quad (22)$$

$$\begin{aligned} U_{\text{eff}}(\rho_A, \rho_B, r) &= \frac{1}{2}\omega^2\left(m_A\rho_A^2 + \frac{1}{2}m_B\rho_B^2 + \frac{1}{2}m_r r^2\right) \\ &+ \frac{\hbar^2(3N_A-4)(3N_A-6)}{8m_A\rho_A^2} + \frac{\hbar^2(3N_B-4)(3N_B-6)}{8m_B\rho_B^2} \\ &+ \langle\Phi_0|V_A|\Phi_0\rangle + \langle\Phi_0|V_B|\Phi_0\rangle + \langle\Phi_0|V_{AB}|\Phi_0\rangle, \end{aligned} \quad (23)$$

where $\langle\Phi_0|V|\Phi_0\rangle$ is the expectation value of the interaction V with the constant angular wave function Φ_0 . With the volume element in equation (11) we find by direct integration

$$\langle\Phi_0|V_A|\Phi_0\rangle = \frac{1}{\sqrt{2\pi}}\frac{\Gamma(\frac{3N_A-3}{2})}{\Gamma(\frac{3N_A-6}{2})}N_A(N_A-1)\frac{\hbar^2 a_A}{m_A\rho_A^3} \quad (24)$$

$$\langle\Phi_0|V_B|\Phi_0\rangle = \frac{1}{\sqrt{2\pi}}\frac{\Gamma(\frac{3N_B-3}{2})}{\Gamma(\frac{3N_B-6}{2})}N_B(N_B-1)\frac{\hbar^2 a_B}{m_B\rho_B^3} \quad (25)$$

$$\begin{aligned} \langle\Phi_0|V_{AB}|\Phi_0\rangle &= \frac{1}{\sqrt{2\pi}}\left(\frac{\Gamma(\frac{3N_A-3}{2})}{\Gamma(\frac{3N_A-6}{2})}\frac{\Gamma(\frac{3N_B-3}{2})}{\Gamma(\frac{3N_B-6}{2})}\right)^{1/2}\frac{\hbar^2 a_{AB}}{2\mu_{AB}(\rho_A\rho_B)^{3/2}} \\ &\times \sqrt{N_A(N_A-1)N_B(N_B-1)}I(\rho_A, \rho_B, r), \end{aligned} \quad (26)$$

where $\Gamma(z)$ is the Gamma function and I is derived in Appendix A as a function of ρ_A , ρ_B and r .

When $N_A \gg 1$ we have $\Gamma(\frac{3N_A-3}{2})/\Gamma(\frac{3N_A-6}{2}) \approx (3N_A/2)^{3/2}$ and analogously for $N_B \gg 1$, see [19]. Then U_{rmeff} is given as

$$U_{\text{eff}} = \frac{1}{2}m_A\omega^2\rho_A^2 + \frac{1}{2}m_B\omega^2\rho_B^2 + \frac{1}{2}m_r\omega^2r^2 + \frac{9N_A^2\hbar^2}{8m_A\rho_A^2} + \frac{9N_B^2\hbar^2}{8m_B\rho_B^2} + \frac{3^{3/2}\hbar^2}{2^2\pi^{1/2}} \left(\frac{N_A^{7/2}a_A}{m_A\rho_A^3} + \frac{N_B^{7/2}a_B}{m_B\rho_B^3} + \frac{(N_A N_B)^{7/4}a_{AB}}{2\mu_{AB}(\rho_A\rho_B)^{3/2}} I(\rho_A, \rho_B, r) \right), \quad (27)$$

which can be considered as the energy surface depending on the three collective coordinates ρ_A , ρ_B and r . The properties of this effective potential then reflects the properties of the solutions which, if necessary, could be computed from the eigenvalue equation (22).

The expression reduces to the one-component potential [4, 20] when $r = 0$ and all particles are identical, i.e.

$$U_{\text{eff}} = \frac{1}{2}m\omega^2\rho^2 + \frac{9N^2\hbar^2}{8m\rho^2} + \frac{3^{3/2}\hbar^2}{2^2\pi^{1/2}} \frac{N^{7/2}a_s}{m\rho^3}, \quad (28)$$

where a_s is the common scattering length and $m = m_A = m_B$.

3. The effective potential

To be specific we consider parameters corresponding to a system where both components are ^{87}Rb atoms with the mass $m_A = m_B = m = 1.44 \times 10^{-25}\text{kg}$ [4]. The bosons in both components are assumed to be trapped in the same spherical harmonic potential with the frequency $\omega = 2\pi \times 23.5\text{Hz}$. The related oscillator length $b_t = \sqrt{\hbar/m\omega}$ is then $2.22 \mu\text{m}$. The particle numbers N_A , N_B and the three s -wave scattering lengths a_A , a_B and a_{AB} are variable parameters.

3.1. The interaction V_{AB}

All terms in the potential (27) are simple and explicitly given, except the function I arising from the interaction V_{AB} in equation (26), see appendix Appendix A. Without this interaction the two subsystems would decouple and each behaves as a separate one-component system. We show this interaction term in figures 1 and 2 for several sets of particle numbers and hyperradii.

The general features are a monotonous function with a flat maximum at $r = 0$ and vanishing exactly for $r > \rho_A + \rho_B$. For given N the symmetric combination of $N_A = N_B$ and $\rho_A = \rho_B$ leads to the highest maximum value of unity corresponding to the smallest average distance between particles in the subsystems A and B . The interaction between the two components is strongest for symmetric systems with coinciding centers. As the centers are moved apart, the interaction becomes larger for different values of ρ_A and ρ_B . Asymmetric division of a given total number of particles also decrease the interaction.

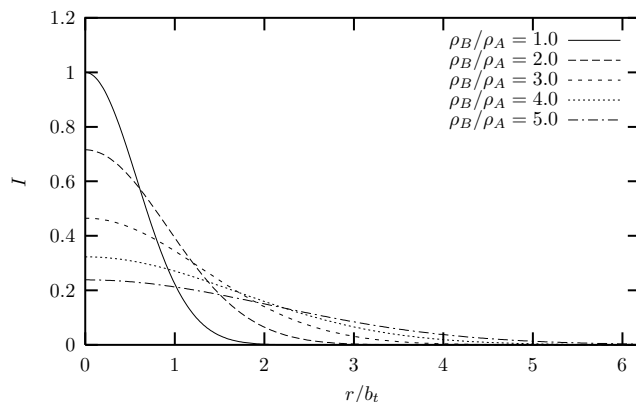


Figure 1. The interaction I defined in equation (26) and Appendix A as function of the distance r between the two centers of masses. The particle numbers are $N_A = N_B = 20000$, $\rho_A = 100b_t$ and the ratios ρ_B/ρ_A are given on the figure.

These properties directly reflect the dependences of the overlap between the two density distributions.

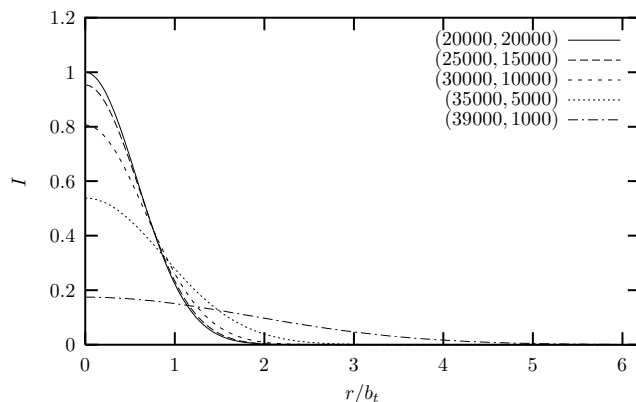


Figure 2. The interaction function I defined in equation (26) and Appendix A as function of the distance r between the two centers of masses for $\rho_A = \rho_B = 100b_t$ and the values of (N_A, N_B) given on the figure.

The two-body interaction strength a_{AB} is a proportionality factor on the function I . Consequently, attraction prefers symmetric division and coinciding centers, whereas repulsion prefers precisely opposite, i.e. asymmetry and large distance between the center of masses.

3.2. Dependence on center of mass distance

We minimize the effective potential in equation (27) with respect to ρ_A and ρ_B for fixed r and given scattering lengths and particle numbers. We first choose interactions corresponding to the two-component condensate of two spin states of ^{87}Rb . The three scattering lengths are then almost identical and given by $a_A = a_B = a_{AB} = 103a_0$ where a_0 is the Bohr radius [4]. The total number of particles is rather arbitrarily fixed to be

$N = N_A + N_B = 40000$. The results for identical scattering lengths are discussed in [22].

The main features are that the effective potential at $r = 0$ is independent of the division of particles N_A and N_B , but still strongly varying with the total number N . This potential value at $r = 0$ is the same as obtained for the one-component potential in equation (28) when ρ is calculated from equation (10) with the minimum values of ρ_A and ρ_B .

For these identical repulsive scattering lengths and the symmetric divisions of $N_B = N_A$, the systems prefer coinciding centers of mass, i.e. the potential has a minimum for $r = 0$. As we increase the particle asymmetry, another minimum appears at $r \approx 2 - 3b_t$ and for $N_B < 0.134N_A$ (or $N_A < 0.134N_B$) eventually becomes deeper. The minimum at $r = 0$ remains, but now separated by a barrier. The deepest of these minima is found when $N_B/N_A \approx 1/40$. Even larger asymmetries again increase the depth and eventually only the $r = 0$ minimum remains as for a one-component system.

Maintaining $a_A = a_B > 0$ we show in figure 3 the variation with the scattering length $a_{AB} > 0$ for a symmetric division of particle numbers. The flat region around $r = 0$ is always present, but the minimum for $a_{AB} \leq a_A$ turns into a maximum when $a_{AB} > a_A$. Then the repulsion between the subsystems is strong enough to move the minimum at $r = 0$ to finite values corresponding to values $r/b_t \approx 3.5 - 4.5$. For less repulsion, $a_{AB} \leq a_A = a_B$, the minimum at $r = 0$ is always present and in addition another minimum at finite r appears for sufficiently asymmetric particle divisions.

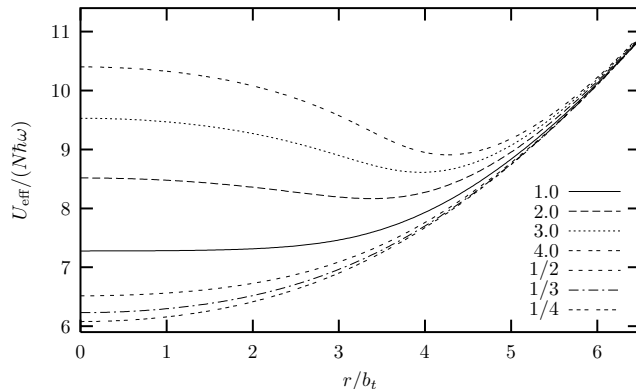


Figure 3. The effective potential in equation (17) as a function of r/b_t for ^{87}Rb masses $m_A = m_B = 1.44 \times 10^{-25}\text{kg}$, trap length $b_t = 2.22\mu\text{m}$ ($\omega = 2\pi \times 23.5\text{ Hz}$), particle numbers $N_A = N_B = 20000$, and $a_A = a_B = 103a_0$, where a_0 is the Bohr radius. The curves correspond to the different values of a_{AB}/a_A given on the figure.

The basic characteristics of a system are size and energy. The root-mean-square distance is the measure of the size of a system which in our coordinates are given by

$$\bar{r}_A^2 = \frac{1}{N_A} \left\langle \sum_{i=1}^{N_A} (\vec{r}_i - \vec{R}_A)^2 \right\rangle = \frac{\langle \rho_A^2 \rangle}{N_A}, \quad (29)$$

$$\bar{r}_B^2 = \frac{1}{N_B} \left\langle \sum_{i=N_A+1}^N (\vec{r}_i - \vec{R}_B)^2 \right\rangle = \frac{\langle \rho_B^2 \rangle}{N_B}, \quad (30)$$

$$\bar{r}^2 = \frac{1}{M} \left\langle \sum_{i=1}^N m_i (\vec{r}_i - \vec{R})^2 \right\rangle = \frac{\langle m \rho^2 \rangle}{M}, \quad (31)$$

where \bar{r} , \bar{r}_A and \bar{r}_B are the root mean square radii for total and individual subsystems and $\langle \rangle$ represents the expectation value for the total wave function.

For identical interactions of $a_{AB} = a_A = a_B$ we found in [22] that $\bar{r}_A = \bar{r}_B = \bar{r} \approx 3b_t$ in the minimum at $r = 0$ independent of particle division. This structure closely resembles the one-component system. Increasing the distance r between the centers of the subsystems reduce all three root mean square radii. However, as N_B/N_A changes, the system with the largest particle number always maintains roughly the same value of about $3b_t$. In contrast, the root mean square radius of the other subsystem decreases to about half of the value for $r = 0$.

The minima of effective potentials as in figure 3 define the preferred structures. The effect of the repulsion is that the two systems try to avoid each other while staying at distances small compared to the size of the confining external field. The large subsystem is exploiting the space almost like it was alone in the trap. When one subsystem is small, it becomes advantageous to place about half of its particles outside the other subsystem. Then the repulsion on the small subsystem from the trap and the other subsystem is minimized.

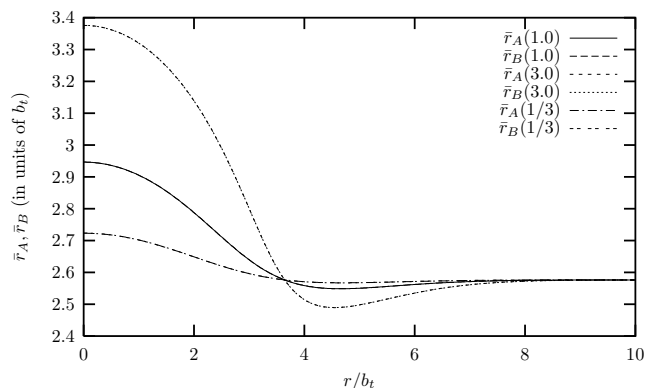


Figure 4. The root-mean-square radii $\bar{r}_A = \bar{r}_B$ as a function of r for some of the systems in figure 3. The curves again correspond to the different values of a_{AB}/a_A given on the figure.

When $N_B < 0.134N_A$, the lowest minimum occurs at finite r . The center of mass of the small system B remains within the radius \bar{r}_A until $N_B \approx 0.004N_A$. For even smaller subsystems the center of B moves a little outside \bar{r}_A , but still the distance between the centers at the minimum remains smaller than $\bar{r}_A + \bar{r}_B$. Therefore, complete separation between the systems does not occur.

Many of these basic properties remain for $0 < a_{AB} \neq a_A = a_B$ as shown in figure 4. The root mean square radii again are largest for $r = 0$ with values increasing as a

function of a_{AB} corresponding to decreasing the overlap in order to decrease the energy. For relatively large values of r where the subsystems essentially can avoid overlapping, the sizes become independent of a_{AB} . At intermediate distances a minimum size is always found. The smaller the repulsion a_{AB} , the less is the variation with center of mass distance.

3.3. Curvature and normal modes

The local minima in the r -direction represent a projection in the three dimensional space. We can evaluate the stability by computing the second derivatives of the effective potential in these points. The kinetic energy operators already only contain second derivatives and the relative Hamiltonian H_{rel} is then to second order approximated by

$$\begin{aligned}
H_{\text{rel}} &\approx U_{\text{eff}}(\rho_{A\text{min}}, \rho_{B\text{min}}, r_{\text{min}}) \\
&\quad - \frac{\hbar^2}{2m_A} \frac{\partial^2}{\partial \rho_A^2} - \frac{\hbar^2}{2m_B} \frac{\partial^2}{\partial \rho_B^2} - \frac{\hbar^2}{2m_r} \frac{\partial^2}{\partial r^2} \\
&\quad + \frac{1}{2} \left(\rho_A - \rho_{A\text{min}}, \rho_B - \rho_{B\text{min}}, r - r_{\text{min}} \right) \\
&\quad \left(\begin{array}{ccc} \left. \frac{\partial^2 U_{\text{eff}}}{\partial \rho_A^2} \right|_{\text{min}} & \left. \frac{\partial^2 U_{\text{eff}}}{\partial \rho_A \partial \rho_B} \right|_{\text{min}} & \left. \frac{\partial^2 U_{\text{eff}}}{\partial \rho_A \partial r} \right|_{\text{min}} \\ \left. \frac{\partial^2 U_{\text{eff}}}{\partial \rho_B \partial \rho_A} \right|_{\text{min}} & \left. \frac{\partial^2 U_{\text{eff}}}{\partial \rho_B^2} \right|_{\text{min}} & \left. \frac{\partial^2 U_{\text{eff}}}{\partial \rho_B \partial r} \right|_{\text{min}} \\ \left. \frac{\partial^2 U_{\text{eff}}}{\partial r \partial \rho_A} \right|_{\text{min}} & \left. \frac{\partial^2 U_{\text{eff}}}{\partial r \partial \rho_B} \right|_{\text{min}} & \left. \frac{\partial^2 U_{\text{eff}}}{\partial r^2} \right|_{\text{min}} \end{array} \right) \begin{pmatrix} \rho_A - \rho_{A\text{min}} \\ \rho_B - \rho_{B\text{min}} \\ r - r_{\text{min}} \end{pmatrix} \quad (32)
\end{aligned}$$

where we used the notation of the 3×3 -matrix sandwiched between the two vectors. All first order derivatives are zero in these minima.

The approximation in equation (32) is almost directly three separable harmonic oscillators. We first redefine the variables by scaling with the related masses as

$$\delta \rho_A \equiv (\rho_A - \rho_{A\text{min}}) \sqrt{m_A \omega / \hbar}, \quad (33)$$

$$\delta \rho_B \equiv (\rho_B - \rho_{B\text{min}}) \sqrt{m_B \omega / \hbar}, \quad (34)$$

$$\delta r \equiv (r - r_{\text{min}}) \sqrt{m_r \omega / \hbar}. \quad (35)$$

Then all three kinetic energy operators are dimensionless and the energy unit is $\hbar \omega$. It is now sufficient to diagonalize the potential matrix in equation (32). The total Hamiltonian then has eigenvalues and eigenvectors λ_i and $\vec{v}_i = (v_i^A, v_i^B, v_i^r)$ for $i = 1, 2, 3$. The total energy is given by $E = \hbar \omega \sum_i^3 (n_i + 1/2) \sqrt{\lambda_i}$ with the non-negative integers n_i corresponding to one-dimensional harmonic oscillators. The excitation energies for each of these vibrational degrees of freedom are then integer multiples of $\hbar \omega \sqrt{\lambda_i}$.

For the minimum at $r = 0$ the ρ_A - ρ_B and the r degrees of freedom decouple completely. This is a consequence of the flat maximum at $r = 0$ for the interaction function in figures 1 and 2, because first order r -derivatives of I then vanish and the only other r -dependence is the r^2 arising from the external field. For this minimum the lowest vibrational r -mode carries the energy $\hbar \omega (n_r + 3/2) \sqrt{\lambda_r}$ dictated by the boundary condition at $r = 0$ corresponding to negative parity. The total energy is in this case

Table 1. Eigenvalues and eigenvectors for the second order harmonic motion in the minimum at $r = 0$ of the effective potential. The eigenvectors ($\tilde{v}_i^A, \tilde{v}_i^B, \tilde{v}_i^r$) refer to the units of root mean square radii or in terms of the initial coordinates $((\rho_A - \rho_{A\min})\sqrt{N_A m_A \omega / \hbar}, (\rho_B - \rho_{B\min})\sqrt{N_B m_B \omega / \hbar}, (r - r_{\min})\sqrt{m_r \omega / \hbar})$. The scattering lengths are $a_{AB} = a_A = a_B = 103a_0$.

N_A	N_B	λ_1	\tilde{v}_1^A	\tilde{v}_1^B	\tilde{v}_1^r	λ_2	\tilde{v}_2^A	\tilde{v}_2^B	\tilde{v}_2^r	λ_3	\tilde{v}_3^A	\tilde{v}_3^B	\tilde{v}_3^r
20000	20000	4.97	0.71	0.71	0.0	2.54	0.71	-0.71	0.0	0.03	0.0	0.0	1.0
32000	8000	4.97	0.97	0.24	0.0	2.54	0.71	-0.71	0.0	0.03	0.0	0.0	1.0
36000	4000	4.97	0.99	0.11	0.0	2.55	0.71	-0.71	0.0	0.03	0.0	0.0	1.0
37000	3000	4.97	1.00	0.08	0.0	2.55	0.71	-0.71	0.0	0.03	0.0	0.0	1.0
39000	1000	4.97	1.00	0.03	0.0	2.55	0.71	-0.71	0.0	0.03	0.0	0.0	1.0
39800	200	4.97	1.00	0.01	0.0	2.56	0.71	-0.71	0.0	0.04	0.0	0.0	1.0

given by $E = \hbar\omega((n_3 + 3/2)\sqrt{\lambda_3} + \sum_{i=1}^2(n_i + 1/2)\sqrt{\lambda_i})$. Still the vibrational excitation energies are integer multiples of $\hbar\omega\sqrt{\lambda_i}$.

The normal modes are given by the components of the eigenvectors \vec{v}_i defining a direction in the coordinate system $(\delta\rho_A, \delta\rho_B, \delta r)$. The physical system has natural length scales for the different degrees of freedom corresponding to the initial coordinates (ρ_A, ρ_B, r) . They are exhibited by the sizes of the subsystems, i.e. the root mean square radii defined in equations (29)-(31). Thus the proper physical length scales are $\rho_A/\sqrt{N_A}$ and $\rho_B/\sqrt{N_B}$, which means that we should multiply the coefficient measuring the ρ_A -component by $\sqrt{N_A}$ to change to the coefficient measuring the corresponding root mean square radius. The normal mode directions with these root mean square unit vectors are then represented by the vectors $(\tilde{v}_i^A, \tilde{v}_i^B, \tilde{v}_i^r) \equiv (v_i^A \sqrt{N_A m_A \omega / \hbar}, v_i^B \sqrt{N_B m_B \omega / \hbar}, v_i^r \sqrt{m_r \omega / \hbar})$.

These eigenvectors and the related eigenvalues are given in tables 1 and 2. For the minimum at $r = 0$ the r -direction is completely decoupled from the two other normal modes mixing ρ_A and ρ_B . By far the lowest eigenvalue corresponds to the r -mode which means vibrations of the relative center of mass.

The next mode is remarkably independent of the particle division, always with exactly equal amplitudes of opposite phase in the A and B root mean square radii. This mode is then an isovector breathing mode where one subsystem shrinks radially while the other radially expands. This vibration is around the equilibrium structure where the subsystems both are of equal size.

The highest-lying mode for the $r = 0$ minimum corresponds to in-phase oscillations of ρ_A and ρ_B . The equal amplitudes of the real size components, $(1, -1) \propto (\tilde{v}_2^A, \tilde{v}_2^B) \propto (v_2^A \sqrt{N_A}, v_2^B \sqrt{N_B})$, combined with orthogonality of (v_1^A, v_1^B) and $(v_2^A, v_2^B) \propto (\sqrt{N_B}, -\sqrt{N_A})$, implies that $(v_1^A, v_1^B) \propto (\sqrt{N_A}, \sqrt{N_B})$, and $(\tilde{v}_1^A, \tilde{v}_1^B) \propto (N_A, N_B)$.

In general, the vector $(v^A, v^B, v^r) \propto (\rho_{A\min} \sqrt{m_A \omega / \hbar}, \rho_{B\min} \sqrt{m_B \omega / \hbar}, r_{\min} \sqrt{m_r \omega / \hbar})$ is at the minimum position precisely in the direction of the total hyperradius defined

Table 2. Eigenvalues and eigenvectors for the second order harmonic motion in the minimum at $r \neq 0$ of the effective potential. The eigenvectors $(\tilde{v}_i^A, \tilde{v}_i^B, \tilde{v}_i^r)$ refer to the units of root mean square radii or in terms of the initial coordinates $((\rho_A - \rho_{A\min})\sqrt{N_A m_A \omega / \hbar}, (\rho_B - \rho_{B\min})\sqrt{N_B m_B \omega / \hbar}, (r - r_{\min})\sqrt{m_r \omega / \hbar})$. The scattering lengths are $a_{AB} = a_A = a_B = 103a_0$.

N_A	N_B	λ_1	\tilde{v}_1^A	\tilde{v}_1^B	\tilde{v}_1^r	λ_2	\tilde{v}_2^A	\tilde{v}_2^B	\tilde{v}_2^r	λ_3	\tilde{v}_3^A	\tilde{v}_3^B	\tilde{v}_3^r
20000	20000	-	-	-	-	-	-	-	-	-	-	-	-
32000	8000	-	-	-	-	-	-	-	-	-	-	-	-
36000	4000	4.97	0.99	0.08	0.08	3.29	0.72	-0.62	-0.31	0.26	0.26	0.49	-0.83
37000	3000	4.97	1.0	0.06	0.06	3.47	0.71	-0.62	-0.34	0.48	0.32	0.51	-0.80
39000	1000	4.97	1.0	0.01	0.02	3.81	0.67	-0.63	-0.40	1.21	0.45	0.50	-0.75
39800	200	4.97	1.0	0.0	0.0	3.90	0.60	-0.67	-0.44	1.77	0.53	0.47	-0.71

in equation (10). For $r = 0$ the root mean square radii of the two subsystems are equal and we have from equations (29)-(31) that $\rho_{A\min}\sqrt{N_B} \approx \rho_{B\min}\sqrt{N_A}$. Thus the highest-lying vibrational mode, $(v_1^A, v_1^B) \propto (\sqrt{N_A}, \sqrt{N_B})$, is exactly in the direction of the hyperradius.

For an equal particle division this is fully the physical breathing mode where both subsystems move in phase with an equal scaling of their radii. For asymmetric particle divisions the largest subsystem tries to breathe like it was alone. The smallest then has to follow as well as possible consistent with orthogonality, which in turn is equivalent to following the ρ -direction. Equal breathing amplitudes are then only consistent with the ρ -direction for a symmetric particle division.

For the minimum at $r \neq 0$ all three directions are mixed in the normal modes as seen in table 2. The lowest-lying energy is now much larger than for the $r = 0$ minimum, but the largest probability is still related to vibration in the r -direction. The second mode again corresponds almost completely to the isovector breathing mode, i.e. out-of-phase oscillation with equal real size amplitudes of the two subsystems. Now an admixture of up to 30% probability in the r -direction is present.

The highest-lying mode is in-phase oscillation of the two subsystems. Again this mode corresponds to maximum variation of the total hyperradius and therefore the breathing mode cannot be fully exploited. The reason is that the largest subsystem determines the mode and tries to oscillate as it was alone in the trap.

For both minima the smallest eigenvalue corresponds essentially to the r -direction. This mode exploits that only the repulsion between A and B is changing when the subsystems maintain their sizes and only move their centers of mass. The second and third eigenvalues are essentially the isovector and isoscalar breathing modes, respectively. The highest vibrational excitation energy, $\hbar\omega\sqrt{\lambda}$, is consistently about $\hbar\omega\sqrt{5}$ which is the one-component result for a Bose-Einstein condensate in the limit of large particle numbers [2]. This breathing mode is energetically less favored than

the isovector breathing mode, where one subsystem oscillates against the other and the repulsive interaction minimizes the overlap. In both these modes all three repulsions contribute.

4. Stability conditions

The stability is first of all determined by the existence of minima. However, for many-body atomic systems lower lying minima certainly exist with structures completely different from condensed states. These metastable states are confined by barriers providing a finite lifetime. In three-dimensional quantum mechanics the minimum in the potential energy may be too shallow or narrow to allow the zero point oscillations. Crude estimates of stability are then first obtained by locating extremum points with positive curvature in the potential. Second by comparing the vibrational energies with the barrier heights.

4.1. The r -mode for identical interactions

Let us first assume identical scattering lengths where two minima in the r -direction appears for some divisions of particles N_A and N_B . The values of the effective potential at these two minima for $r = 0$ and $r \neq 0$ are shown in figure 5. The first prominent feature is that only the $r = 0$ -minimum exists for $N_B/N_A > 5400/34600 \sim 0.156$. For more asymmetric divisions, $N_B/N_A < 4712/35288 \sim 0.134$, the minimum at finite r quickly becomes substantially deeper.

The zero point energies are added to the potential, but the sum coincides with the potential within the thickness of the lines in figure 5. Both oscillations are essentially always classically allowed, i.e. around finite r very quickly after it appeared and around $r = 0$ until the asymmetry reaches very small values.

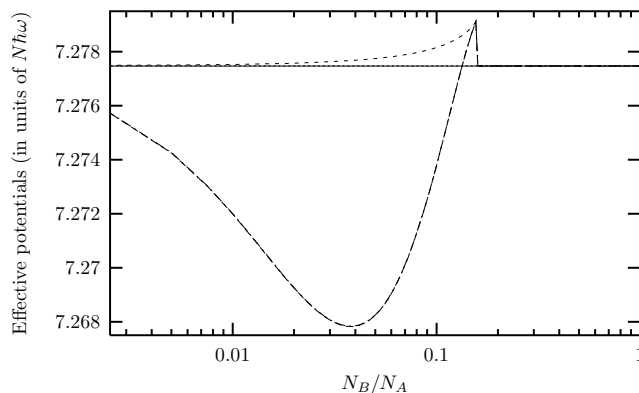


Figure 5. The values of the effective potential at the extremum points as a function of N_B/N_A for $N_A + N_B = 40000$ and $a_A = a_B = a_{AB} = 103a_0$. We show the minima at $r = 0$ (solid line) and $r \neq 0$ (long-dashed line), and the separating maximum (short-dashed line). The zero point energies, added to the effective potentials, are also shown for both minima, $r = 0$ (dotted line) and $r \neq 0$ (dot-dashed line).

The highest minimum located at $r = 0$ could in principle decay into the lowest minimum at finite r . The related lifetime can be estimated by the WKB tunneling approximation where the decay rate Γ/\hbar is given by

$$\Gamma/\hbar = \frac{\omega_r}{\pi} \exp\left(-\frac{2}{\hbar} \int_{r_2}^{r_1} dr \sqrt{2m_r(U_{\text{eff}}(r) - U_{\text{eff}}(r=0) - 3\hbar\omega_r/2)}\right), \quad (36)$$

where r_1 and r_2 are the turning points and $\omega_r = \omega\sqrt{\lambda_r}$ is the oscillation frequency in the r -direction. These decay rates are computed and shown in figure 6 for the $r = 0$ minimum for the cases exhibited in figure 5. The lifetime increases dramatically as the systems become more asymmetric. Only when N_B/N_A is close to 0.001, the rate becomes comparable to the frequency of the trap. For example for $N_B/N_A \approx 0.0025$ the rate $\Gamma/(\hbar\omega) \approx 8 \times 10^{-9}$.

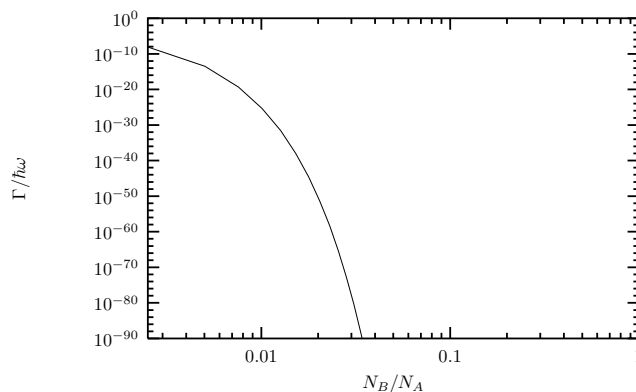


Figure 6. The WKB decay rate defined in equation (36) as function of N_B/N_A for the minimum at $r = 0$ for the cases in figure 5.

The structures in these minima are reflected by the root mean square radii defined in equations (29)-(31). For $r = 0$ all these sizes are equal. For finite r we show the results in figure 7 for the same parameters as in figure 5. The largest system maintains the same size $\bar{r}_A \approx 3b_t$ independent of particle number. The size of the smallest system decreases with increasing asymmetry. In all cases we find that $\bar{r}_A + \bar{r}_B > r$, i.e. complete separation between systems never occurs. Furthermore, $\bar{r}_A > \bar{r}$ when $N_B/N_A > 150/39850 \sim 0.004$, i.e. the center of mass of the small system remains within the radius of the large system except for very asymmetric particle divisions.

4.2. The r -mode for symmetric particle division

The stability of the r -mode changes with the three interactions. For $r = 0$ the condition for instability against separation of the two center of masses is a negative curvature in the minimum of the effective potential in the r -direction. We restrict ourselves to $m_A = m_B = m$, $N_A = N_B$ and $a_A = a_B$ and define the coordinate at the potential minimum by $\rho_{A\text{min}} = \rho_{B\text{min}}$. This minimum point is determined as the zero point of the

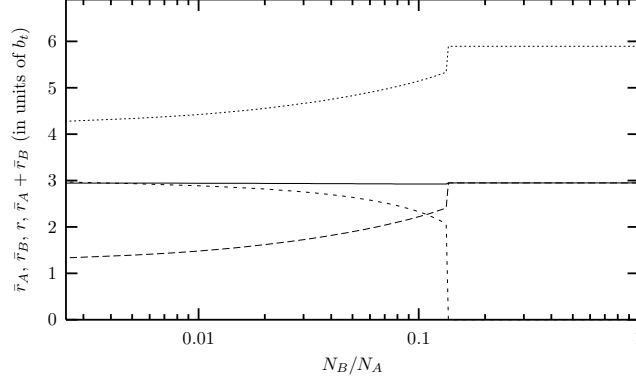


Figure 7. The root mean square radii \bar{r}_A (solid), \bar{r}_B (long-dashed), r (short-dashed) and $\bar{r}_A + \bar{r}_B$ (dotted) for the minimum at finite r shown in figure 5. The minimum at $r = 0$ has $\bar{r}_A = \bar{r}_B \approx 3b_t$ which also is shown for the most symmetric systems.

first derivative, i.e. $\frac{\partial U_{\text{eff}}}{\partial \rho_A}|_{r=0} = 0$, which is equivalent to

$$f(\rho_A) \equiv \left[m\omega^2 \rho_A^5 - \frac{9 N_A^2 \hbar^2}{4 m} \rho_A - \frac{3^{5/2} N_A^{7/2} \hbar^2}{4\sqrt{\pi} m} (a_A + a_{AB}) \right] = 0, \quad (37)$$

with precisely one solution $\rho_{\text{Amin}}/b_t \geq (3N_A/2)^{1/2} 5^{-1/4}$ when $N_A(a_A + a_{AB})/b_t \geq -(8\pi)^{1/2} 5^{-5/4}$. Furthermore, the function $f(\rho_A)$ is positive for $\rho_A > \rho_{\text{Amin}}$.

A negative curvature, $\frac{\partial^2 U_{\text{eff}}}{\partial r^2}|_{r=0} < 0$, is then equivalent to

$$\rho_A^5 < \frac{3^{5/2} N_A^{7/2} \hbar^2 a_{AB}}{2\pi^{1/2} m^2 \omega^2} \equiv \rho_{Ac}^5 \quad (38)$$

The instability condition, $(3N_A/2)^{1/2} 5^{-1/4} b_t \leq \rho_{\text{Amin}} < \rho_{Ac}$, is equivalent to the inequality $f(\rho_{Ac}) > 0$, which in turn is equivalent to the two simultaneous conditions

$$\frac{a_A}{b_t} < \frac{a_{AB}}{b_t} - \frac{\pi^{2/5}}{2^{1/5} N_A^{4/5}} \left(\frac{a_{AB}}{b_t} \right)^{1/5}, \quad (39)$$

$$\frac{N_A a_{AB}}{b_t} > \frac{\pi^{1/2}}{2^{3/2} 5^{5/4}}. \quad (40)$$

When $a_A = a_B = 0$ the critical repulsion derived from equation (40) corresponds to $a_{AB}/b_t = \frac{\sqrt{\pi}}{2^{1/4} N_A}$. For finite values of $a_A = a_B > 0$ the critical value of a_{AB} has to be correspondingly increased. The behavior of the effective potential is illustrated in figure 3 for parameter combinations close the critical values for separation of the two centers of mass. The potentials are rather flat and the minimum therefore quickly moves to separation distances comparable to the trap length.

4.3. Stability of the ρ_A and ρ_B -modes

Qualitative understanding can be reached by analytic investigations for symmetric systems, i.e. $N_A = N_B$, $a_A = a_B$ with the constraint $r = 0$. Then the condition that the effective potential at $r = 0$ has no stationary point, $\frac{\partial U_{\text{eff}}}{\partial \rho_A}|_{r=0} \neq 0$ for any

coordinates ρ_A and ρ_B , can be expressed as

$$\frac{N_A(a_A + a_{AB})}{b_t} \leq -\frac{2^{3/2}\pi^{1/2}}{5^{5/4}} \sim -0.67. \quad (41)$$

Then the two-component system is unstable since collapse to a point is unavoidable.

Stability requires, beside a stationary point, also that the curvature is positive in all directions. Then the eigenvalues of the curvature matrix must all be positive at the stationary point. For $r = 0$ we then construct and diagonalize the matrix

$$\begin{pmatrix} \frac{\partial^2 U_{\text{eff}}}{\partial \rho_A^2} & \frac{\partial^2 U_{\text{eff}}}{\partial \rho_A \partial \rho_B} \\ \frac{\partial^2 U_{\text{eff}}}{\partial \rho_B \partial \rho_A} & \frac{\partial^2 U_{\text{eff}}}{\partial \rho_B^2} \end{pmatrix}. \quad (42)$$

For $\rho_A = \rho_B$ we can compute the eigenvalues analytically and find the conditions expressing when at least one of them is negative and the point therefore unstable. In Appendix B we derive these conditions, i.e. the system is unstable when the following two inequalities both are satisfied

$$\frac{a_{AB}}{b_t} \leq -\frac{5^5 N_A^4}{2^8 \pi^2} \left(\frac{a_A}{b_t}\right)^5 + \frac{1}{4} \frac{a_A}{b_t}, \quad (43)$$

$$\frac{N_A a_A}{b_t} \leq -\frac{2^{3/2} \pi^{1/2}}{5^{5/4}}. \quad (44)$$

The last inequality, the stability condition for the A -component alone, can be obtained both in the mean-field approximation and with hyperspherical coordinates [1, 2, 19]. Furthermore, equation (44) is obtained from equation (43) for non-interacting subsystems, where $a_{AB} = 0$. Both equations (41) and (43) can be derived in the mean field approximation [18].

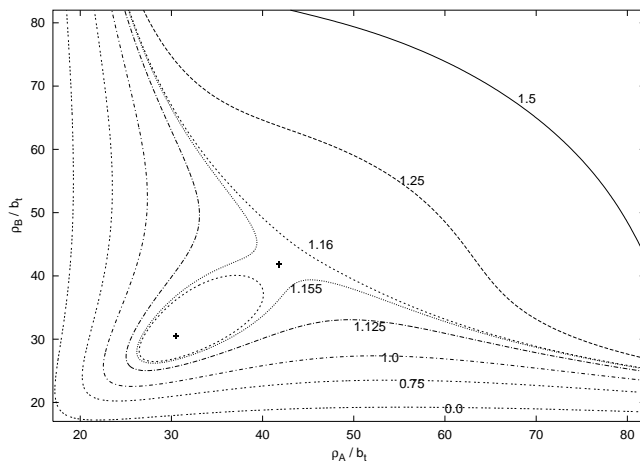


Figure 8. Contour plot of the potential $U_{\text{eff}}/(N\hbar\omega)$ in equation (27) as a function of ρ_A and ρ_B for $r = 0$, $N_A = N_B = N/2 = 2000$, $a_{AB} = 0.0001b_t$, and $a_A = a_B = -0.00042b_t$.

These conditions are most easily visualized by two-dimensional contour diagrams of the effective potential as function of ρ_A and ρ_B with $r = 0$. Such a diagram is shown in figure 8 for interactions very close to the critical values given in equations

(43) and (44). The potential increases when either ρ_A or ρ_B individually become large. This effect of the external field is especially clearly seen along the line $\rho_A = \rho_B$, where the potential decreases from large values at very large distances, proceeds through a minimum located at around $42b_t$ to reach a maximum at about $30b_t$, and finally decreases to $-\infty$ at the origin. However, the minimum along this line is in fact a saddle point and therefore unstable as soon as both degrees of freedom are included. From the saddle point the energy decreases in the “isovector” direction where the sum of ρ_A and ρ_B remains constant.

This saddle point changes into a stable minimum with slightly larger repulsion between the two subsystems as illustrated in figure 9. The same qualitative behavior is seen along the $\rho_A = \rho_B$ line, where the minimum and maximum are shifted to positions further apart at about $48b_t$ and $20b_t$, respectively. Also the regions at relatively large distances along the coordinate axes are essentially unchanged. In the “isovector” direction, as well as in all other directions, the potential now increases as characteristic for a minimum. However, the minimum is very shallow and only a small amount of energy would destabilize the system.

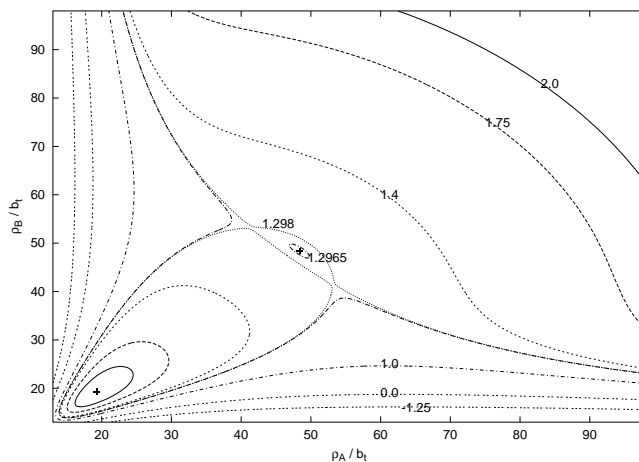


Figure 9. Contour plot of the potential $U_{\text{eff}}/(N\hbar\omega)$ in equation (27) as a function of ρ_A and ρ_B for $r = 0$, $N_A = N_B = N/2 = 2000$, $a_{AB} = 0.0002b_t$, and $a_A = a_B = -0.00042b_t$.

4.4. Phase diagram of stability

We are now in a position to discuss the stability for different interactions. We consider again equal particle division while independently varying the scattering lengths $a_A = a_B < 0$ and a_{AB} . The numerically computed stability diagram is shown in figure 10. We shall discuss the different regions in this contour plot in comparison with the analytic derivation.

First, we consider two attractive subsystems, $a_{AB}/b_t \leq 0$, where the coinciding centers are preferred. The computed stability condition then follows the expression in equation (41), which for $a_{AB} = 0$ reduces to the one-component stability condition.

Thus, the attraction between A and B reduces the stability region. It is amusing that $a_A = a_B = 0$ leads to the apparently identical stability condition of $N_A a_{AB}/b_t > -0.67$. However, since $N_A = N_B$ now the total number of pair interactings is twice as large, i.e. N_A^2 compared to $N_A^2/2$.

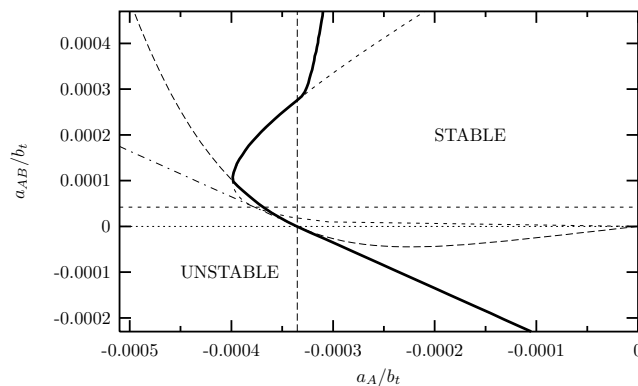


Figure 10. Stability regions for a two-component system with $N_B = N_A = 2000$ as a function of $a_A = a_B < 0$ and a_{AB} . The thick solid line separates stable (right side) from unstable (left side) regions when we allow three degrees of freedom, i.e. ρ_A , ρ_B , and r . The different curves are related to equations (41) (dot-dashed), (43) and (44) (long-dashed), (39) and (40) (short-dashed), respectively.

For relatively small repulsion, $0 < a_{AB}/b_t \lesssim 0.0001$, the stability follows the expression in equation (43). This corresponds to a local, but unstable minimum at $r = 0$, since equation (44) then also is obeyed. These conditions are related to structures of coinciding centers and therefore they are the same as derived from the mean-field approximation [18].

For larger repulsion, $0.0001 \lesssim a_{AB}/b_t$, separate center of masses of the two systems are energetically favored. The condition for separation is given in equation (40) which follows the computed stability curve in the interval $0.0001 \lesssim a_{AB}/b_t < 0.0003$. The substantial reduction of the region of mean-field stable solutions is then defined by the difference between the curves described by equations (40) and (43).

For larger repulsion $a_{AB}/b_t > 0.0003$ the stable region is larger than found from equation (40), because the structure at finite r is stable for relatively strong repulsion between the subsystems. This repulsion has the effect of squeezing each of the subsystems more than if they had been left alone as described by equation (41). Then the stable region in figure 10 is in fact smaller than for non-interacting subsystems, because the barrier preventing collapse now is circumvented by the energetically favored smaller sizes and the finite r . Each subsystem therefore finds itself with values of $\rho_{A\min}$ and $\rho_{B\min}$ on the unstable side of the barrier preventing collapse if each were left alone. The mutual repulsion destabilizes the total system compared to separate subsystems.

5. Conclusions

We use hyperspherical coordinates to describe a mixture of two different components each consisting of identical bosons. Sufficiently dilute and spatially extended systems can be rather well approximated by use of only s -waves for all relative angular momenta. From far apart only the monopole part of the interactions is important and this is reflected in the wave function. We are then left with a wave function only depending on the most important coordinates, i.e. the hyperradius for each subsystem and the distance between the two center of masses.

With a wave function depending on these three collective coordinates and three-dimensional δ -functions as the two-body interactions we derive the corresponding Schrödinger equation and compute the effective potential. The behavior of this potential and the external field as a function of the three collective coordinates are decisive for the properties of the two-component system. Several features are similar to results from the mean-field approximation. We used the simplest non-trivial assumptions and leave lots of room for improvements. Especially two-body correlations could be included in the wave function and finite range two-body interactions with the correct behavior could be employed.

When the interaction between particles in the two subsystems is attractive, the potential has a minimum for coinciding centers of mass. Then the stable structures are quite similar to those obtained with the mean-field approximation. When the repulsion is sufficiently strong, new stable structures arise with finite distance between the centers. Asymmetric particle numbers in the subsystems favor these structures. For moderate repulsion two stable structures are simultaneously present for centers coinciding and at a finite distance.

New vibrational modes appear. The three normal modes essentially correspond to relative center of mass motion with the lowest energy, isovector and isoscalar motion with out-of-phase and in-phase oscillations of the two subsystems as the second and third mode, respectively. Only the highest-lying isoscalar vibration is present in one-component systems, where the excitation energy of $\sqrt{5}$ times the energy quantum of the harmonic trap almost precisely is found in our computations.

New stability conditions are established. The relative center of mass degree of freedom provides both more stable structures and reduced stability compared to mean-field calculations. Even when the independent subsystems are marginally stable, a comparably strong repulsion between the subsystems destabilizes the total system.

In conclusion, new features arise for two-component systems, i.e. different stable structures, excitation modes, and stability conditions.

Appendix A. The interaction V_{AB}

We want to compute the expectation value of the interaction V_{AB} in equation (5) over all angles, i.e. all coordinates except ρ_A , ρ_B and r . We assume that the constant angular

wave function Φ_0 is normalized in the corresponding space, i.e. $\int d\Omega |\Phi_0|^2 = 1$, where $d\Omega \equiv d\Omega_r d\Omega_{N_A-1} \int d\Omega_{N_B-1}$ with the notation from equation (11) precisely defined in [20]. The boson symmetry implies that this expectation value is

$$\begin{aligned} \langle \Phi_0 | V_{AB} | \Phi_0 \rangle &= g_{AB} \int d\Omega \sum_{i=1}^{N_A} \sum_{j=N_A+1}^N \delta^{(3)}(\vec{r}_i - \vec{r}_j) |\Phi_0|^2 \\ &= g_{AB} N_A N_B |\Phi_0|^2 \int d\Omega \delta^{(3)}(\vec{r}_{N_A} - \vec{r}_{N_B}), \end{aligned} \quad (\text{A.1})$$

where the position vectors can be expressed by center of mass coordinates and Jacobi vectors $\vec{\eta}$, i.e.

$$\vec{r}_{N_A} = \vec{R}_A + \sqrt{\frac{N_A-1}{N_A}} \vec{\eta}_{N_A-1} \quad (\text{A.2})$$

$$\vec{r}_{N_B} = \vec{R}_B + \sqrt{\frac{N_B-1}{N_B}} \vec{\eta}_{N_B-1}. \quad (\text{A.3})$$

With $\vec{r}_{N_A} - \vec{r}_{N_B} \equiv \vec{r}_\eta - \vec{r}$, we need the δ -function in spherical coordinates, i.e.

$$\delta^{(3)}(\vec{r}_\eta - \vec{r}) = \frac{\delta(r_\eta - r)}{r_\eta r} \sum_\ell \frac{2\ell + 1}{4\pi} P_\ell(\cos \theta), \quad (\text{A.4})$$

where $P_\ell(\cos \theta)$ are Legendre polynomials, θ is the angle between \vec{r}_η and \vec{r} , and $r_\eta = |\vec{r}_\eta|$. We then get

$$\langle \Phi_0 | V_{AB} | \Phi_0 \rangle = g_{AB} N_A N_B |\Phi_0|^2 \int d\Omega_{N_A-1} d\Omega_{N_B-1} \frac{\delta(r_\eta - r)}{r_\eta r}, \quad (\text{A.5})$$

where r_η can be rewritten, by using $\eta_{N_A-1} = \rho_{N_A-1} \sin \alpha_{N_A-1}$ and $\eta_{N_B-1} = \rho_{N_B-1} \sin \alpha_{N_B-1}$, as

$$\begin{aligned} r_\eta^2 &= \frac{N_A-1}{N_A} \rho_A^2 \sin^2 \alpha_{N_A-1} + \frac{N_B-1}{N_B} \rho_B^2 \sin^2 \alpha_{N_B-1} \\ &\quad - 2 \sqrt{\frac{N_A-1}{N_A}} \sqrt{\frac{N_B-1}{N_B}} \rho_A \rho_B \sin \alpha_{N_A-1} \sin \alpha_{N_B-1} \cos \theta_{AB} \end{aligned} \quad (\text{A.6})$$

where θ_{AB} is the angle between $\vec{\eta}_{N_A-1}$ and $\vec{\eta}_{N_B-1}$.

By changing integration variable from θ_{AB} to $x \equiv r_\eta - r$ we arrive at equation (26) where the reduced interaction is defined by

$$I = \frac{\bar{I}}{r} \frac{4N_A N_B (\rho_A \rho_B)^{1/2}}{(N_A-1)(N_B-1)} \left(\frac{2\Gamma(\frac{3N_A-3}{2})\Gamma(\frac{3N_B-3}{2})}{\pi\Gamma(\frac{3N_A-6}{2})\Gamma(\frac{3N_B-6}{2})} \right)^{1/2} \quad (\text{A.7})$$

in terms of the basic integral

$$\begin{aligned} \bar{I}(\rho_A, \rho_B, r) &\equiv \int d\alpha_{N_A-1} \sin \alpha_{N_A-1} \cos^{3N_A-7} \alpha_{N_A-1} \\ &\quad \times \int d\alpha_{N_B-1} \sin \alpha_{N_B-1} \cos^{3N_B-7} \alpha_{N_B-1} \\ &\quad \times \Theta(r_\eta^{(+)} - r) \Theta(r - r_\eta^{(-)}) \end{aligned} \quad (\text{A.8})$$

where Θ is the Heaviside function and

$$\begin{aligned} r_\eta^{(\pm)} &= \left| \sqrt{\frac{N_A - 1}{N_A}} \rho_A \sin \alpha_{N_A - 1} \pm \sqrt{\frac{N_B - 1}{N_B}} \rho_B \sin \alpha_{N_B - 1} \right| \\ &\approx |\rho_A \sin \alpha_{N_A - 1} \pm \rho_B \sin \alpha_{N_B - 1}|, \end{aligned} \quad (\text{A.9})$$

where we from now on shall use the last approximation valid for $N_A \gg 1$ and $N_B \gg 1$.

For further derivation we treat separately various cases of different relative sizes ρ_A , ρ_B and r . The resulting closed analytic expressions are one-dimensional integrals of simple functions of the angle α , i.e.

$$f_\pm(\rho_A, \rho_B, r, \alpha) \equiv \frac{\sin \alpha}{3N_B - 6} \cos^{3N_A - 7} \alpha \left[1 - \frac{(r \pm \rho_A \sin \alpha)^2}{\rho_B^2} \right]^{(3N_B - 6)/2}. \quad (\text{A.10})$$

The integration limits are defined by the functions

$$g_\pm(\rho_A, \rho_B, r) \equiv \arcsin[|r \pm \rho_B|/\rho_A]. \quad (\text{A.11})$$

We distinguish between a number of cases.

1. $[2\rho_B < \rho_A \text{ and } 0 \leq r < \rho_B]$ or $[\rho_B \leq \rho_A < 2\rho_B \text{ and } 0 \leq r < \rho_A - \rho_B]$:

$$\bar{I}(\rho_A, \rho_B, r) = \int_0^{g_+} f_- - \int_0^{g_-} f_+. \quad (\text{A.12})$$

2. $2\rho_B < \rho_A$ and $\rho_B \leq r < \rho_A - \rho_B$:

$$\bar{I}(\rho_A, \rho_B, r) = \int_{g_-}^{g_+} f_-. \quad (\text{A.13})$$

3. $2\rho_B < \rho_A$ and $\rho_A - \rho_B \leq r < \rho_A + \rho_B$:

$$\bar{I}(\rho_A, \rho_B, r) = \int_{g_-}^{\pi/2} f_-. \quad (\text{A.14})$$

4. $2\rho_B < \rho_A$ and $\rho_A + \rho_B \leq r$:

$$\bar{I}(\rho_A, \rho_B, r) = 0. \quad (\text{A.15})$$

5. $\rho_B \leq \rho_A < 2\rho_B$ and $\rho_A - \rho_B \leq r < \rho_B$:

$$\bar{I}(\rho_A, \rho_B, r) = \int_0^{\pi/2} f_- - \int_0^{g_-} f_+. \quad (\text{A.16})$$

6. $\rho_B \leq \rho_A < 2\rho_B$ and $\rho_B \leq r < \rho_A + \rho_B$:

$$\bar{I}(\rho_A, \rho_B, r) = \int_{g_-}^{\pi/2} f_-. \quad (\text{A.17})$$

The cases not covered are obtained by interchanging ρ_A and ρ_B .

The limit of $r = 0$ is obtained by expansion. We first assume $\rho_A > \rho_B$

$$\frac{1}{r} \bar{I} \sim \left. \frac{\partial \bar{I}}{\partial r} \right|_{r=0} + \frac{r^2}{6} \left. \frac{\partial^3 \bar{I}}{\partial r^3} \right|_{r=0} \quad (\text{A.18})$$

$$\begin{aligned} \left. \frac{\partial \bar{I}}{\partial r} \right|_{r=0} &= \frac{2\rho_A}{\rho_B} \int_0^{\arcsin(\rho_B/\rho_A)} d\alpha \sin^2 \alpha \\ &\times \cos^{3N_A - 7} \alpha \left[1 - \frac{\rho_A^2}{\rho_B^2} \sin^2 \alpha \right]^{(3N_B - 8)/2} \end{aligned} \quad (\text{A.19})$$

$$\begin{aligned} \left. \frac{\partial^3 \bar{I}}{\partial r^3} \right|_{r=0} &= -6(3N_B - 8) \frac{\rho_A}{\rho_B^4} \int_0^{\arcsin(\rho_B/\rho_A)} d\alpha \sin^2 \alpha \\ &\times \cos^{3N_A-7} \alpha \left[1 - \frac{\rho_A^2}{\rho_B^2} \sin^2 \alpha \right]^{(3N_B-10)/2} \end{aligned} \quad (\text{A.20})$$

$$\begin{aligned} &+ 2(3N_B - 8)(3N_B - 10) \frac{\rho_A^3}{\rho_B^6} \int_0^{\arcsin(\rho_B/\rho_A)} d\alpha \sin^4 \alpha \\ &\times \cos^{3N_A-7} \alpha \left[1 - \frac{\rho_A^2}{\rho_B^2} \sin^2 \alpha \right]^{(3N_B-12)/2}, \end{aligned} \quad (\text{A.21})$$

where $\left. \frac{\partial^2 \bar{I}}{\partial r^2} \right|_{r=0} = 0$. The expressions for $\rho_B > \rho_A$ are found by interchanging.

Appendix B. Stability of ρ -modes

When we assume $m_A = m_B = m$, $N_A = N_B$, $\rho_A = \rho_B$ and $r = 0$ the eigenvalues for the matrix in equation (42) are simply $\frac{\partial^2 U_{\text{eff}}}{\partial \rho_A^2} \pm \frac{\partial^2 U_{\text{eff}}}{\partial \rho_A \partial \rho_B}$. The lowest eigenvalue is negative when

$$g(\rho_A) \equiv m\omega^2 + \frac{27N_A^2}{4} \frac{\hbar^2}{m\rho_A^4} + \frac{3^{5/2}N_A^{7/2}}{\pi^{1/2}} \frac{\hbar^2}{m\rho_A^5} \left(a_A - \frac{a_{AB}}{4} \right) \leq 0 \quad (\text{B.1})$$

for the solution $\rho_A = \rho_{A\text{min}}$ obtained from equation (37). This is never possible when $a_A \geq a_{AB}/4$ and the then the system is always stable. When $a_A < a_{AB}$ we continue by subtracting the function $f(\rho_{A\text{min}}) = 0$ in equation (37) from the inequality in equation (B.1). This immediately leads to

$$\frac{(3N_A/2)^{1/2}}{5^{1/4}} \leq \rho_{A\text{min}} \leq -\frac{5 \cdot 3^{1/2} N_A^{3/2} a_A}{2^2 \pi^{1/2} b_t} \equiv \rho_{Ab}, \quad (\text{B.2})$$

where we added the inequality for the lowest possible value of $\rho_{A\text{min}}$. Then $g(\rho_{Ab}) < 0$ is the condition for instability, which by simple insertion results in equation (43). Using instead the lower limit in equation (B.2) we arrive at condition (44) which is the stability condition for a one-component system.

References

- [1] Pethick C J and Smith H 2001 *Bose-Einstein Condensation in Dilute Gases* (Cambridge: Cambridge University Press)
- [2] Pitaevskii L and Stringari S 2003 *Bose-Einstein Condensation* (Oxford: Clarendon Press)
- [3] Myatt C J *et al* 1997 *Phys. Rev. Lett.* **78** 586
- [4] Hall D S *et al* 1998 *Phys. Rev. Lett.* **81** 1539
- [5] Maddaloni P *et al* 2000 *Phys. Rev. Lett.* **85** 2413
- [6] Modugno G *et al* 2002 *Phys. Rev. Lett.* **89** 190404
- [7] Truscott A G *et al* 2001 *Science* **291** 2570
- [8] Schreck F *et al* 2001 *Phys. Rev. Lett.* **87** 080403
- [9] Roati G *et al* 2002 *Phys. Rev. Lett.* **89** 150403
- [10] Modugno G *et al* 2002 *Science* **297** 2240
- [11] Hadzibabic Z *et al* 2002 *Phys. Rev. Lett.* **88** 160401
- [12] Chui S T and Ao P 1999 *Phys. Rev. A* **59** 1473

- [13] Esry B D and Greene C H 1999 *Phys. Rev. A* **59** 1457
- [14] Gordon D and Savage C M 1998 *Phys. Rev. A* **58** 1440
- [15] Pu H and Bigelow N P 1998 *Phys. Rev. Lett.* **80** 1134
- [16] Öhberg P 1999 *Phys. Rev. A* **59** 634
- [17] Svidzinsky A A and Chui S T 2003 *Phys. Rev. A* **68** 013612
- [18] Busch Th *et al* 1997 *Phys. Rev. A* **56** 2978
- [19] Bohn J L *et al* 1998 *Phys. Rev. A* **58** 584
- [20] Sørensen O *et al* 2002 *Phys. Rev. A* **66** 032507
- [21] Sørensen O *et al* 2002 *Phys. Rev. Lett.* **89** 173002
- [22] Sogo T *et al* 2004 submitted for publication (*Preprint cond-mat/0402271*)
- [23] Sørensen O *et al* 2004 *J. Phys. B* **37** 93
- [24] Sørensen O *et al* 2003 *Phys. Rev. A* **68** 063618